Article

A cryptic site in class 5 epitope of SARS-CoV-2 RBD maintains highly conservation across natural isolates

Neutralization potency of mAb 6D6 unchanged to various SARS-CoV-2 variants

6D6

D614G

XBB.1.5   BQ.1.1

Neutralization

MAb 6D6 conferred therapeutic efficacy against Beta variant challenge in hamsters

Beta

Probability of Survavil

Body Weight Change

6D6 epitope located in a highly conserved site

(99.92% in all SARS-CoV-2 isolates)

Lingyan Cui,
Tingting Li, Miaolin
Lan, ..., Ying Gu,
Ningshao Xia,
Shaowei Li

litingting@xmu.edu.cn (T.L.)
guying@xmu.edu.cn (Y.G.)
shaowei@xmu.edu.cn (S.L.)

Highlights
6D6 maintains broad-spectrum effectiveness against multiple SARS-CoV-2 variants

6D6 retains consistent neutralization against highly mutated BQ and XBB sublineages

6D6 shows full protection against the virulent Beta variant in hamster model

6D6 site in class 5 epitope remains 99.92% conserved across SARS-CoV-2 isolates
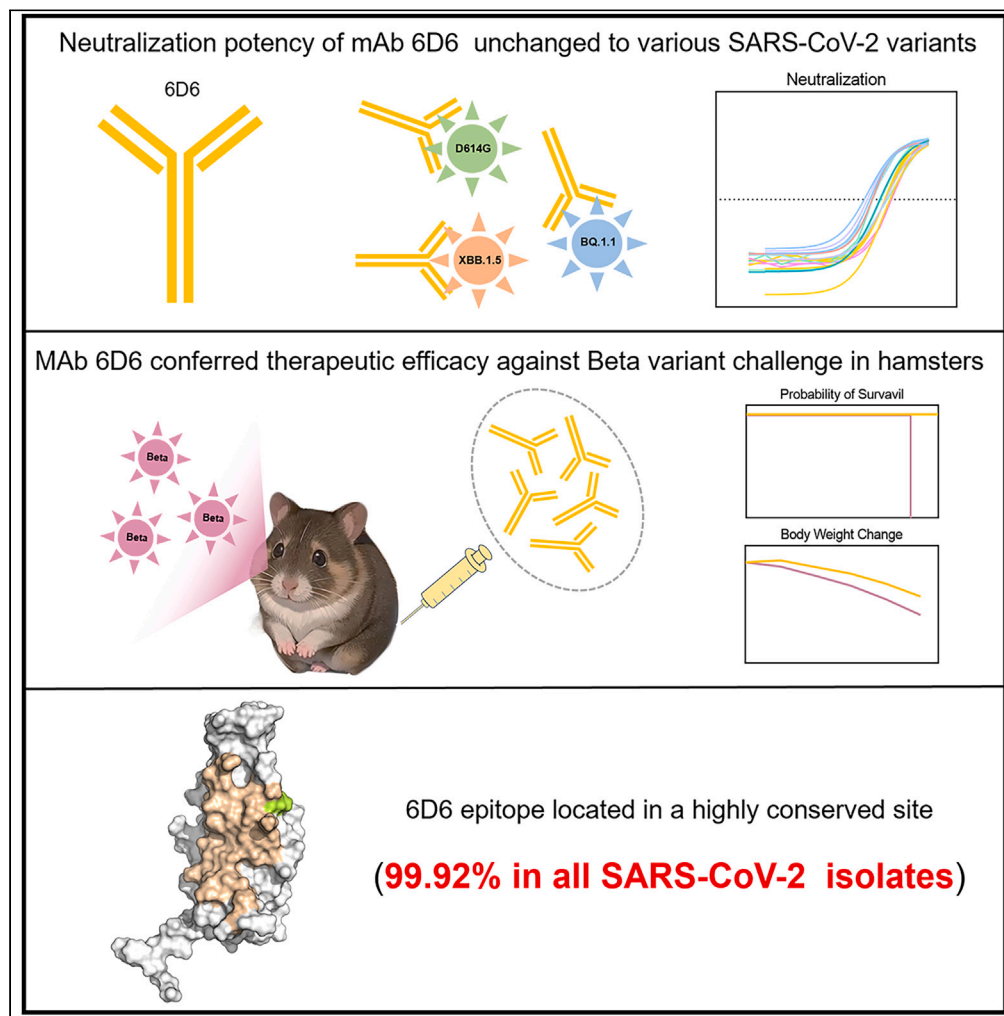
Article

A cryptic site in class 5 epitope of SARS-CoV-2 RBD maintains highly conservation across natural isolates

Lingyan Cui,[1,2,5] Tingting Li,[1,2,5,*] Miaolin Lan,[1,2,5] Ming Zhou,[1,2,5] Wenhui Xue,[1,2] Sibo Zhang,[1,2] Hong Wang,[1,2] Minqing Hong,[1,2] Yali Zhang,[1,2] Lunzhi Yuan,[1,2] Hui Sun,[1,2] Jianghui Ye,[1,2] Qingbing Zheng,[1,2] Yi Guan,[3,4] Ying Gu,[1,2,*] Ningshao Xia,[1,2] and Shaowei Li[1,2,6,*]

SUMMARY

The emergence of SARS-CoV-2 variants raises concerns about the efficacy of existing COVID-19 vaccines and therapeutics. Previously, we identified a conserved cryptic class 5 epitope of SARS-CoV-2 receptor binding domain (RBD) by two cross-neutralizing antibodies 7D6 and 6D6. Intriguingly, this site remains resistant to substantial mutations occurred in ever-changing SARS-CoV-2 subvariants. As compared to class 3 antibody S309, 6D6 maintains broad and consistent neutralizing activities against SARS-CoV-2 variants. Furthermore, 6D6 effectively protected hamster from the virulent Beta strain. Sequence alignment of approximately 6 million documented SARS-CoV-2 isolates revealed that 6D6 epitope maintains an exceptionally high conservation rate (99.92%). Structural analysis demonstrated that all 33 mutations accumulated in XBB.1.5 since the original strain do not perturb the binding 6D6 to RBD, in line with the sequence analysis throughout the antigenicity evolution of SARS-CoV-2. These findings suggest the potential of this epitope serving as a critical determinant for vaccines and therapeutic design.

INTRODUCTION

The recent outbreak coronavirus disease 2019 (COVID-19), caused by severe acute respiratory syndrome coronavirus 2 (SARS-CoV-2), has resulted in severe illness and fatalities worldwide. Notably, COVID-19 represents the third major coronavirus outbreak, following the epidemics caused by SARS-CoV and Middle East respiratory syndrome coronavirus (MERS-CoV).[1] The first case of SARS-CoV-2 infection, dating back to late 2019, has rapidly spread worldwide, posing a significant threat to public health.[2] In response, the World Health Organization (WHO) declared COVID-19 a global public health emergency.[3] As of May 15, 2023, the WHO has reports over 766 million infections and 6.9 million deaths globally (https://www.who.int/).

Vaccination is a crucial strategy in combating the COVID-19 pandemic. Numerous vaccine candidates have been developed, with the WHO reporting 183 candidates in preclinical studies and 199 in clinical evaluation as of March 30, 2023. However, the ongoing evolution of SARS-CoV-2 variants raises concerns about the efficacy of vaccine-induced immunity, particularly with significant vaccine efficiency loss noted in the Beta and Omicron variants.[4–6] Several approaches are being explored to develop novel vaccines to combat potential immune escape of SARS-CoV-2 variants, such as combination of different vaccines or designing broad-spectrum or multivalent vaccines. On August 23, 2021, the Food and Drug Administration (FDA) and the European Medicines Agency (EMA) authorized emergency use of the BNT162b2 bivalent vaccine (Pfizer–BioNTech) that targets both the Omicron BA.4-5 spike (BA.4 and BA.5 encode an identical spike protein) and the ancestral wild-type (D614G) spike of SARS-CoV-2. Data indicated that additional BNT162b2 dose induced potent neutralization against Omicron variant that was low-to-absent in primary series vaccines.[7] Additionally, SCTV01E, a recombinant S-trimer protein antigen developed by SinoCellTech, has shown enhanced neutralization against various SARS-CoV-2 variants, including Omicron subvariants.[8] Nevertheless, recent BQ and XBB subvariants demonstrate a heightened ability to evade neutralizing antibodies, even in individuals vaccinated with the bivalent mRNA booster or previously infected with Omicron.[9] Monoclonal antibodies (mAbs) and convalescent plasma have shown potential in

treating COVID-19 caused by the original SARS-CoV-2 strain. Specially, an antibody cocktail therapy included tixagevimab and cilgavimab to treat COVID-19 patients, including immunocompromised subjects, has demonstrated a substantial reduction in hospital admissions in phase 3 clinical trials.[10] The administration of neutralizing antibodies is valuable given the frequent lack of humoral response to vaccination in immunocompromised patients. However, Omicron lineage variants have reduced the effectiveness of previously approved antibody-based therapy, such as S309, moreover, the efficiency of REGN10933 was completely nullified.[11–13] Moreover, both BQ and XBB are fully resistant to LY-CoV1404 (Bebtelovimab), thereby leaving no clinically authorized therapeutic antibodies effective against these circulating variants.[9]

The Spike (S) protein of SARS-CoV-2, essential for viral entry into host cells, is the primary neutralizing target.[14,15] The currently known anti-SARS-CoV-2 antibodies predominantly target the RBD and are classified into classes 1–5 based on epitope specificity.[16–18] The epitopes of RBD-targeting antibodies in class 1 and class 2 overlap with the ACE2 footprint on the RBD, and they achieve neutralizing by directly blocking ACE2 binding. However, common mutations in the RBD, such as K417N, E484K, N501Y, and Q493R, causes most of these antibodies to lose their neutralizing abilities for variants such as Beta, Gamma, and Omicron.[19] Class 3 and class 4 antibodies bind the outside the ACE2-binding region, with their epitopes being more conserved in the RBD.[20] Nonetheless, the Omicron mutations are situated within the binding site of all four epitopes targeted by mAbs.[21] The newly emerged subvariants BQ.1 and BQ.1.1 are largely pan-resistant to antibodies targeting the RBD class 1 and class 3 epitopes, whereas XBB and XBB.1 are pan-resistant to antibodies targeting the RBD class 1, 2, and 3 epitopes.[9] XBB.1.5 with a rare mutation F486P, has shown superior transmissibility and immune escape ability compared to other subvariants, becoming the dominant strain in several countries.[22] Class 5 mAbs, recently described, bind to a conserved region of the RBD and show potential broad neutralizing abilities, as demonstrated by 7D6/6D6,[23] COVOX-45,[24] and S2H97.[18] It was reported that positioning of the class 5 mAb when bound to the RBD prompts greater conformational rearrangements in the S trimer, ultimately influencing neutralization potency and breadth of mAbs that target related epitopes.[23,25] S2H97 bind to a highly conserved epitope on RBD and could neutralize BA.1 variant. This antibody can bind to with high affinity to 45 RBDs of SARS-related coronaviruses, indicating its promise as a neutralizing agent.[26] While the potential expanse of COVOX-45 is still undergoing investigation, it may deliver broad protection by utilizing a similar neutralization mechanism given its recognition of an epitope similar to S2H97. The class 5 mAbs represent an attractive target for immunogen design and broad-spectrum vaccine development.

With over 50 significant mutations in the SARS-CoV-2 S protein, Omicron has demonstrated remarkable resistant to class 1, 2, 3, and 4 RBD antibodies.[27] Emerging subvariants have accumulated new mutations, further evading neutralizing antibody immunity. Our previous work identified two cross-neutralizing antibodies, 6D6 and 7D6, targeting a unique site on the RBD. 7D6 and 6D6 showed robust binding activity against wild-type RBD and its mutants harboring earlier dominant mutations at N501Y, K417N/E484K/N501Y, L452R. Remarkably, these two antibodies exhibited extraordinarily potent broad-neutralization against pseudoviruses of the prevalent SARS-CoV-2 variants B.1.1.7, B.1.351, and P.1 and the authentic B.1.351 virus.[23] Owing to minor discrepancies in the binding angles and accessibility of epitopes between the two antibodies, 6D6 demonstrates a higher affinity to the Spike trimer as compared to 7D6. Moreover, 6D6 conferred stronger effectiveness than 7D6 in neutralization assays, in particular, showed 5-fold higher in the authentic B.1.351 virus neutralization.[23] Therefore, we chose 6D6 as the promising candidate for further investigation. In this study, we performed an exhaustive evaluation and comparison of 6D6 with a collection of representative antibodies, including previously reported monoclonals like S309, REGN10933, and CB6, which have shown high inhibitory activity against several emerging SARS-CoV-2 variants. We elaborated on the properties of 6D6, which has been proven to neutralize a spectrum of variants including BQ and XBB subvariants, and maintain a virtually unchanged broad-spectrum neutralization capacity against all pseudotyped variants tested. Furthermore, 6D6 exhibited significant protective effects in a hamster model exposed to the Beta variant, evidenced by a considerable reduction in infectious virus load relative to the control group. Sequence analysis and epitope mapping indicates that diverse mutations in SARS-CoV-2 pandemic do not affect the epitope recognized by 6D6, underscoring its potential in next-generation antibody therapies and broad-spectrum vaccine development against SARS-CoV-2.

RESULTS

Construct design, expression, and purification of different S-6P proteins and mAbs

To assess the binding and neutralizing activity range of 6D6 against SARS-CoV-2, we constructed several SARS-CoV-2 and SARS-CoV S-6P proteins. These sequences, including D614G, B.1.621 (Mu), C.1.2, B.1.617.2 (Delta), B.1.1.529 (Omicron), BA.2, B.1.640.1, XBB.1.5, and SARS-CoV, were obtained from the GISAID (https://www.gisaid.org/). A trimerization foldon was added to the C-terminus of the S-6P, and the proteins were further engineered with mutations, including six Pro substitutions (817, 892, 899, 942, 986, and 987), and a "GSAS" replacement at the furin cleavage site (residues 682–685). The coding genes were cloned into the pcDNA3.4 vector with the addition of a His tag, and a FLAG tag (Figure 1A). All S-6P protein types eluted in the separation fractions were presented at molecular weights (m.w.) of ~180 kDa in SDS-PAGE and showed high purity (>95%) (Figure 1B). The expression level of S-6P protein in different mutant strains varies, likely due to mutation-induced property changes. All mAbs were resolved at molecular weights (m.w.) of 50 kDa heavy chains and 25 kDa light chains in SDS-PAGE and showed a high purity (Figure 1C).

Binding capability of 6D6 to SARS-CoV-2 variants S-6P proteins

A comparative evaluation of several antibodies was carried out to examine the binding efficacy of 6D6 to the spike protein. Enzyme-linked immunosorbent assay (ELISA) demonstrated that 6D6 continually exhibited strong binding potential with all the nine tested S-6P proteins, including Omicron subvariants. This was evidenced by half-maximal effective concentration (EC$_{50}$) values ranging between 2.9 and 40.0 ng/mL (Figure 2A). It was observed that S309 maintained potent binding activity across most S-6P proteins except for a 10-fold decrease for B.1.1529 and BA.2. On the other hand, CB6 and REGN10933, displayed significantly reduced reactivities toward B.1.159, BA.2, XBB.1.5,
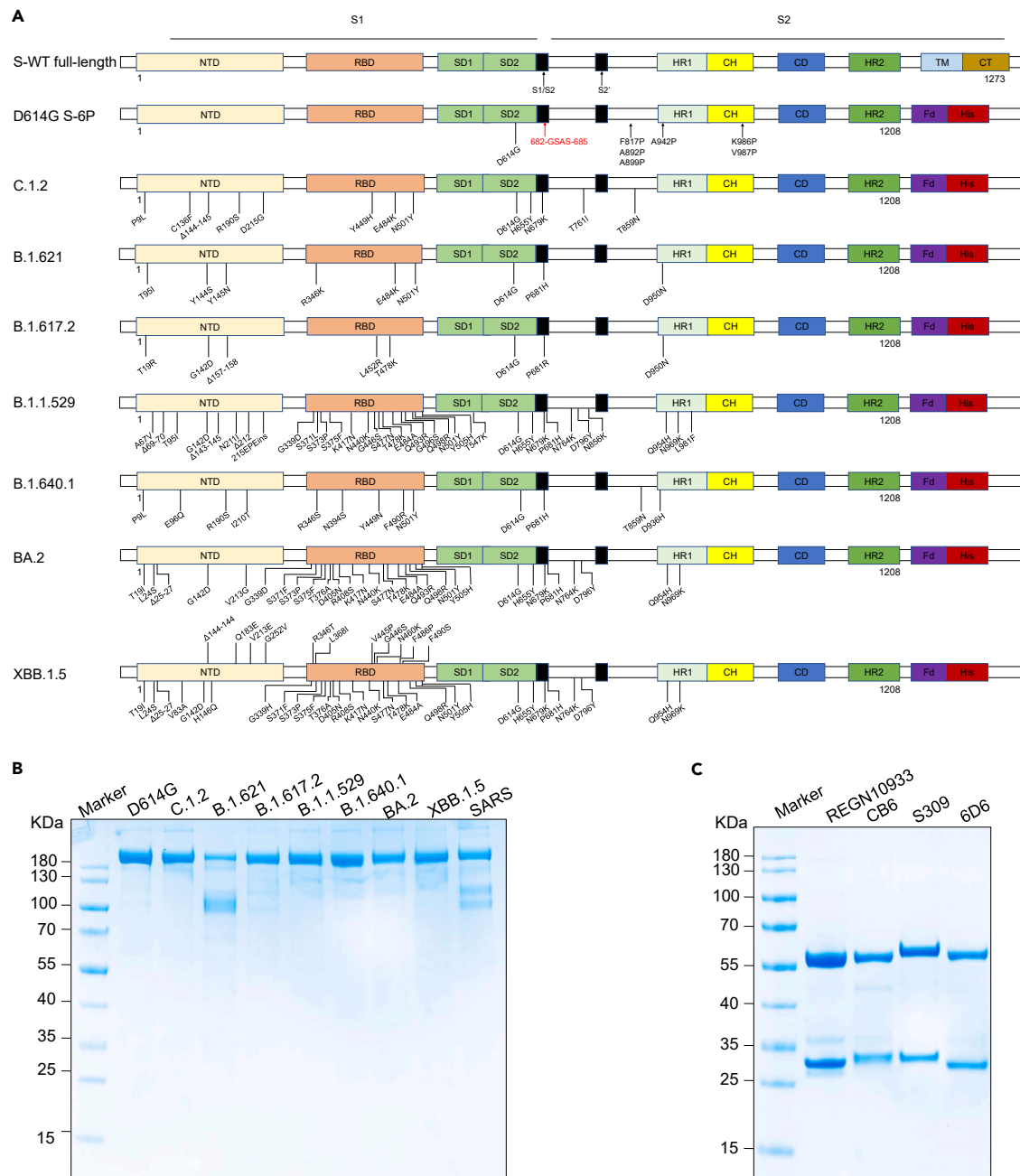
Figure 1. The purification of SARS-CoV-2 S-6P protein and mAbs

(A) Schematic representation of the Spike protein structure, highlighting key domains including the N-terminal domain (NTD), receptor binding domain (RBD), subdomains 1 and 2 (SD1, SD2), heptad repeats 1 and 2 (HR1, HR2), central helix (CH), connector domain (CD), transmembrane domain (TM), cytoplasmic tail (CT), alongside the T4 foldon motif (FD).

(B) SDS-PAGE image of proteins purified via Ni-NTA. The S-6P protein was eluted using 250 mM imidazole.

(C) SDS-PAGE of mAbs purified from protein A agarose columns.

and SARS-CoV. Surface plasmon resonance (SPR) analysis corroborated these findings, demonstrating that both 6D6 and S309 have nanomolar affinities toward diverse viral variants (Figures 2B and S1). Notably, affinity of 6D6 was superior by approximately one logarithmic unit to S309 for SARS-CoV and Omicron lineage variants. Moreover, REGN10933 and CB6 showed minimal response toward B.1.159, BA.2, XBB.1.5, and SARS-CoV, a result that is mirrored by the ELISA. In conclusion, 6D6 displayed exceptional binding reactivity to both SARS-CoV-2 variants and SARS-CoV, reacting with all tested S-6P trimers. This was particularly evident with high affinity toward the Omicron lineage.

A
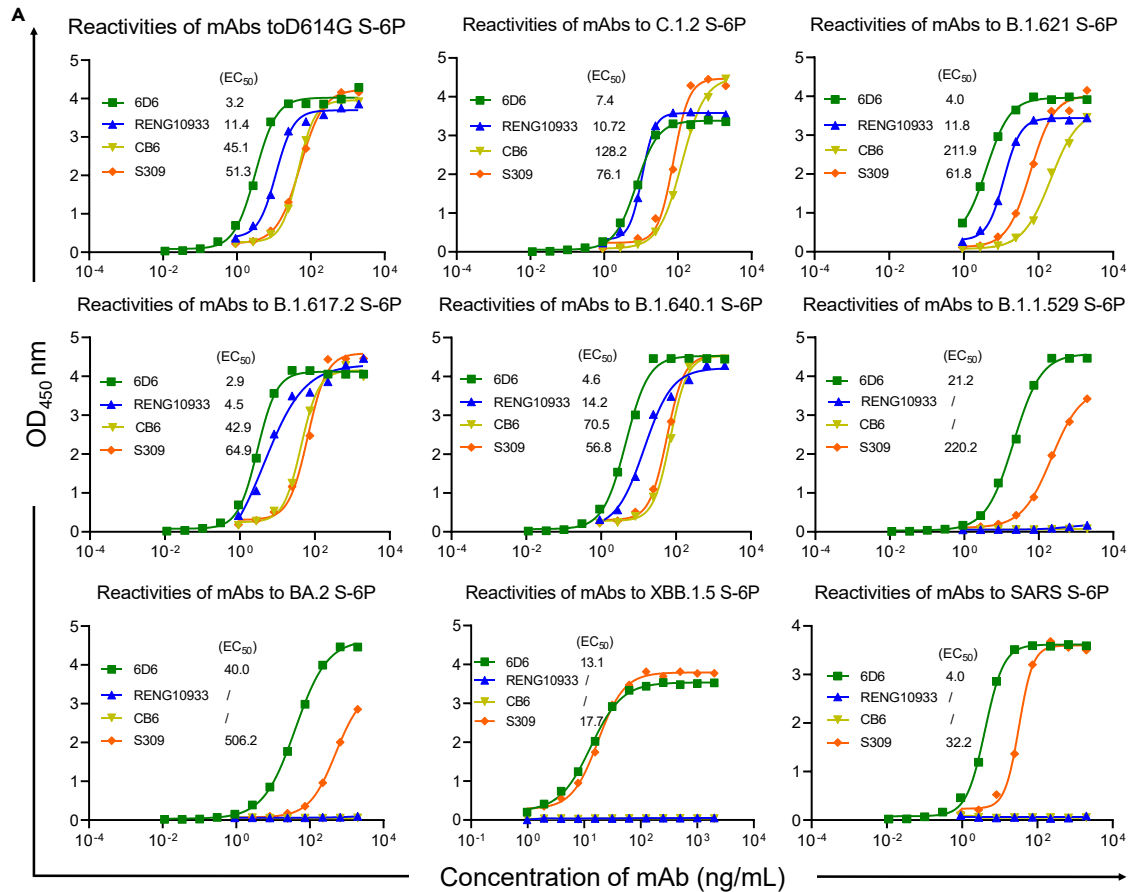
B

Binding affinity of mAbs to S-6P proteins (K_D, nM)

Target	6D6	CB6	S309	RENG10933
D614G S-6P	0.002	1.22	0.0002	0.62
C.1.2 S-6P	0.06	6.50	0.002	0.02
B.1.621 S-6P	0.15	0.61	0.01	0.002
B.1.617.2 S-6P	1.46	5.53	2.01	0.06
B.1.640.1 S-6P	0.11	2.33	0.08	0.15
B.1.1.529 S-6P	8.98	ND	29.90	ND
BA.2 S-6P	0.005	ND	8.17	ND
XBB.1.5 S-6P	0.004	ND	0.04	ND
SARS S-6P	0.008	ND	0.02	ND

Figure 2. The characterization of mAb 6D6

(A) ELISA-based assessment of binding capabilities of 6D6 and other antibodies against various SARS-CoV-2 variants.

(B) Surface Plasmon Resonance (SPR) affinities of mAbs to S-6P proteins from SARS-CoV-2 variants and SARS-CoV. Non-detectable interactions are marked as "ND".

Broad neutralizing activity of 6D6

With the continuous emergence of new viral mutants, particularly the wide prevalence of Omicron, certain mutants exhibit stronger immune evasion abilities. For further examination, we assessed the cross-neutralization potential of 6D6 and S309 using lentiviral virus (LV) pseudotyping systems. The 6D6 showed neutralizing activity against all 14 tested variants, including D614G, B.1.617.1, B.1.617.2, BA.1, BA.1.1, BA.2,

A

B

C

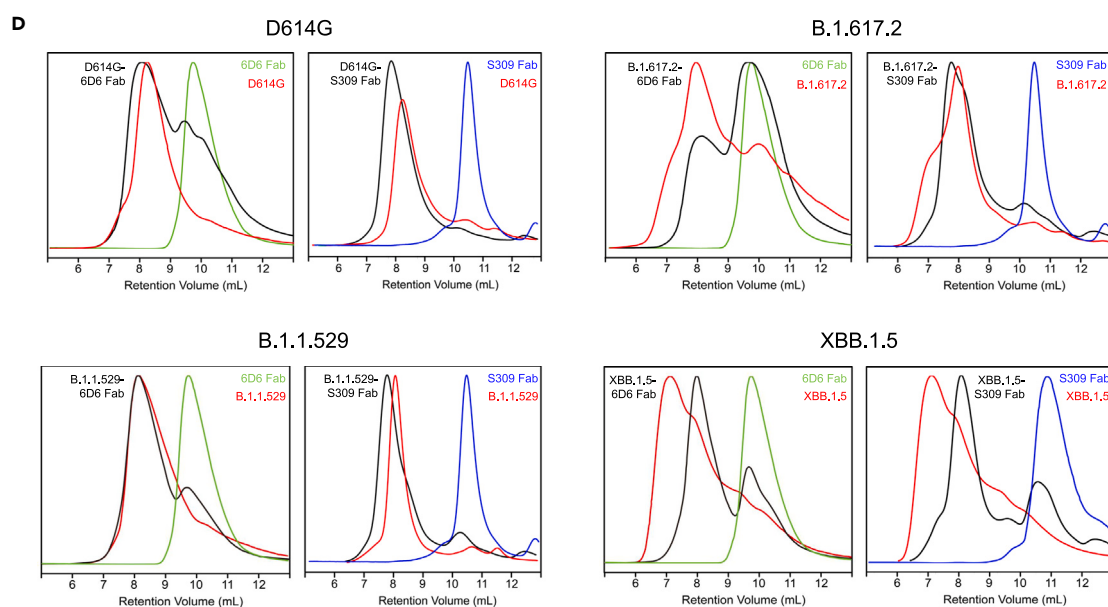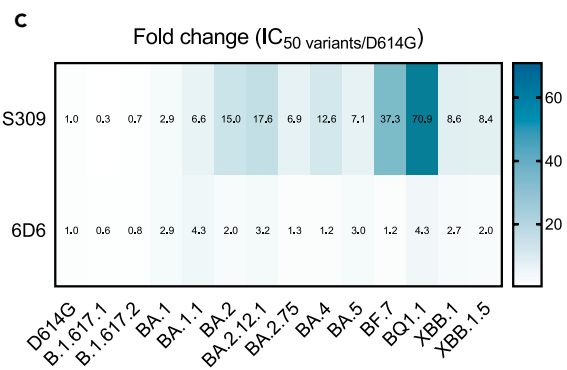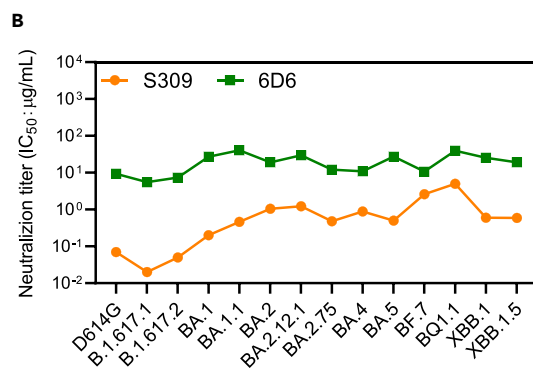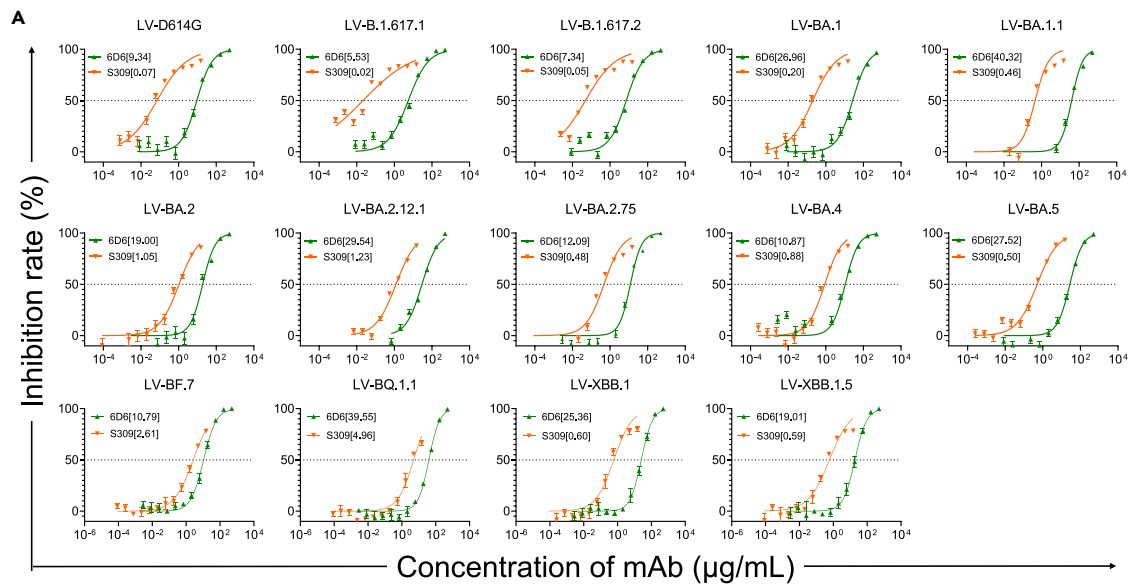Fold change (IC$_{50}$ variants/D614G)

D

Figure 3. Broad neutralization activity of 6D6 against SARS-CoV-2 variants

(A) Neutralization potency of 6D6 and S309 against various SARS-CoV-2 variants, including Omicron, using an LV pseudovirus system. The graph shows IC_{50} values for D614G, B.1.617.1, B.1.617.2, BA.1, BA.1.1, BA.2, BA.2.12.1, BA.2.75, BA.4, BA.5, BF.7, BQ.1.1, XBB.1, XBB.1.5.

(B) Comparison of neutralization potency changes of nAbs against SARS-CoV-2 variants, with IC_{50} values from (A). S309 is represented in orange, and 6D6 in green.

(C) Numbers in the box indicate the fold-change value, and the blue color indicates more change in neutralizing potency.

(D) HPLC profiles of 6D6 and S309 binding to the S trimer of different variants. The red peak is S trimer. The blue peak is S309 Fab. The green peak is 6D6 Fab. The black peak indicates depolymerization of the spike.

BA.2.12.2, BA.2.75, BA.4, BA.5, BF.7, BQ.1.1, XBB.1, XBB.1.5, with IC_{50} value ranging from 5.53 to 41.93 μg/mL. S309 also exhibited potent cross-neutralization, with an IC_{50} value ranging from 0.02 to 11.18 μg/mL (Figure 3A). The neutralizing activity of 6D6 and S309 exhibits varying degrees of damage to different variants. On average, the neutralizing activity of 6D6 was lower than that of S309 (Figures 3A and 3B). However, the decrease in neutralization for S309 relative to D614G was more than 10-fold for BA.2, BA.2.12.1, BA.4, BF.7, BQ.1.1, XBB.1, and XBB.1.5, particularly with a 37.3-fold decrease in BF.7 and a 70.9-fold decrease in BQ.1.1. In contrast, 6D6 demonstrated comparable broad-spectrum neutralization against all tested pseudotyped variants, including recent BF.7, BQ.1.1, XBB.1, and XBB.1.5 subvariants (change within 5-fold) (Figures 3B and 3C). In all, although 6D6 generally demonstrated lower neutralizing activity than S309, it exhibited consistent broad-spectrum neutralization across all tested pseudotyped variants, which may be related to its recognition of conserved epitope.

Our previous studies confirmed that 6D6 mediates neutralization by disrupting the trimeric spike of SARS-CoV-2. Here, we examined binding of 6D6 Fab and S309 Fab to S-6P variants in vitro by incubating excess Fab with S-6P trimers and then flowing through high-performance liquid chromatography (HPLC). HPLC analysis showed delayed retention volume or reduced peak height of complexes (9.5 mL) after equivalent S-6P (7–8 mL) of D614G, B.1.617.2, B.1.1.529, XBB.1.5 incubated with 6D6 Fab (10 mL), which indicated S-6P trimer were dissociated into smaller components. Additionally, when S309 Fab (10.5 mL) was co-incubated with S-6P, dissociation of the S trimer of XBB.1.5 (9.5 mL) was observed except for D614G, B.1.617.2, and B.1.1.529 complexes (7–8 mL) (Figure 3D). These results are consistent with our previously reported neutralization mechanism for 6D6 by antibody-induced spike disruption. And S309 Fab specifically bind to other variants of S-6P, without causing trimer dissociation, which may possibly neutralize the virus via induction of spike trimer cross-linking, steric hindrance, aggregation of virions, and/or inhibition of viral membrane attachment via C-type lectin receptors[13,28] (Figure 3D). Based on the result, it is evident that 6D6 is capable of dissociating the S-6P trimer in different SARS-CoV-2 variants, and supports the mechanism of broad-spectrum neutralization.

Therapeutic activities of 6D6 against SARS-CoV-2 Beta variant challenge in hamsters

The Beta variant exhibits the high resistance to neutralization of sera sourced from both vaccinated individuals and convalescent serum.[29] Infections with the Beta variant are associated with a greater intensity of disease, leading to life-threatening conditions, and a higher rate of COVID-19-related fatalities, as compared to the Alpha variant (B.1.1.7).[30] The therapeutic activity of 6D6 against the Beta variant infection was evaluated utilizing a hamster model (Figure 4A). Eight-week-old male hamsters were intranasally inoculated with 1×10^4 plaque-forming units (PFU) of the Beta variant, and were subsequently treated with an intraperitoneal injection of 6D6, totaling a dose of 20 mg/kg, a day after the infection (dpi). The untreated control group witnessed a 15.7% average loss in body weight, and totally succumbed within a week of infection. In contrast, 6D6-treated hamsters showed only a 10.2% average weight loss with no fatalities (Figures 4B and 4C). Viral load was quantified in respiratory tract tissues (nasal turbinate, trachea, proximal and distal lung zones) via RT-PCR targeting the ORF1ab and nucleoprotein N genes. The viral RNA concentration in the untreated group rose to approximately 10^7-10^9 copies/mL in lung tissues, while 6D6 treatment significantly reduced these levels to about 10^5-10^7 copies/mL. Encouragingly, 6D6 substantially reduced viral RNA quantities in the nonlung respiratory tract—such as the nasal turbinate and trachea—and halted virus replication in lung tissues (Figure 4D). This potential of 6D6 to reduce the viral load in the upper respiratory tract could prove beneficial in lowering the risk of SARS-CoV-2 transmission across populations. Protective efficacy of 6D6 against viral infection-related lung damage was also evaluated. For the untreated group, severe pathological changes, such as multifocal diffuse hyperemia and consolidation, were observed. In comparison, treatment with 6D6 conspicuously curtailed the appearance of such lesions (Figure 4E). Overall, these findings illustrate that the potent neutralization capacity of 6D6 effectively protects hamsters from Beta variant infection and correlated lung damage.

Sequence and structural analysis of 6D6's broad neutralization of SARS-CoV-2 variants

The progression of the pandemic, especially post the emergence of the Omicron variant, has been marked by several antigenic mutations in the spike RBD, enhancing the virus's survival and evasion capabilities. We analyzed spike protein sequences from various pandemic stages, as available in the GISAID and NGDC database, focusing on amino acid substitutions in the RBD. We identified two distinct mutation waves: the "RBD wave" encompassing earlier sequences and the "Omicron wave." Notably, Omicron subvariants, particularly XBB.1.5, have accumulated a high number of RBD mutations, include G339H, R346T, F486P, F490S, etc, raising concerns about current vaccine and effectiveness of mAb therapies (Figure 5A). To date, SARS-CoV-2 variants of concerns (VOCs) rarely mutate near class 5 antigenic sites. Sequence analysis showed that the frequency of mutation in the 6D6 epitope was extremely low (conservation: 99.92% in all SARS-CoV-2 strains, N = 5,960,320; 99.51% in SARS-CoV-2 VOCs, N = 6,573,403; 99.68% in Omicron, N = 3,376,575; 86.67% in Sarbecovirus, N = 5,960,403) (Figure 5B; Table S1). In July 2021, we reported the conservation of 6D6 epitope in SARS-CoV-2 is >99.7% (N = 2,216,094), these data indicated that the 6D6 epitope
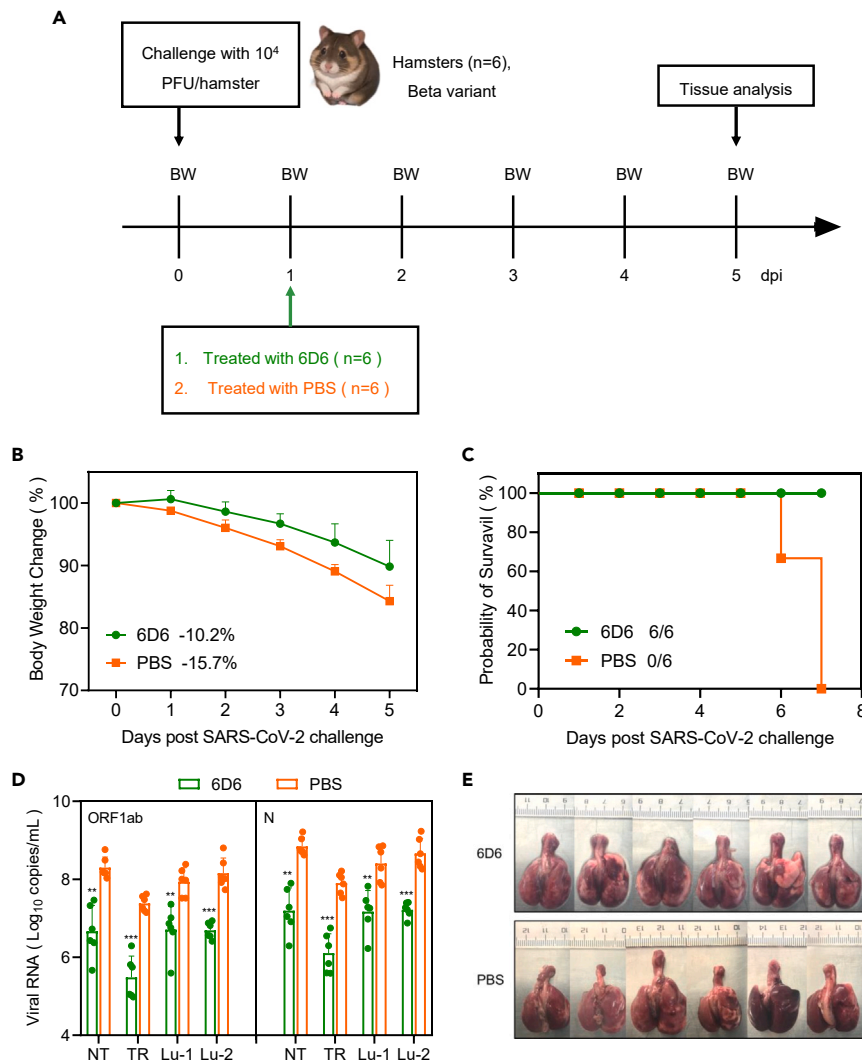
Figure 4. Therapeutic efficacy of 6D6 against SARS-CoV-2 Beta variant in hamsters

(A) Experimental Scheme: A group of 12 male hamsters, divided evenly into two groups, were intranasally infected with the SARS-CoV-2 Beta variant at 1 × 10⁴ PFU. Subsequently, these animals were intraperitoneally treated with either a total dose of 20 mg/kg of 6D6 or PBS as a control at 1 dpi. Daily body weight measurements were taken and lung samples were collected for examination at 5 dpi.

(B) Graph demonstrating changes in body weight induced by virus challenge are presented. Data are expressed as means ± SEM. Significant differences between groups were evaluated using Student's unpaired two-tailed t test.

(C) Illustrates the number of surviving hamsters.

(D) Indicate concentrations of viral RNA in lysates obtained from nasal turbinate (NT), trachea (TR), and lung regions proximal (Lu-1) and distal (Lu-2) to the pulmonary hilum. Data are expressed as means ± SEM. Significant differences between groups were analysed by two-way ANOVA with Bonferroni's multiple comparisons test. *: $p < 0.05$; **: $p < 0.01$; ***: $p < 0.001$; ****: $p < 0.0001$.

(E) Gross observations of lung tissues following the therapeutic.

remained highly conserved during the evolution of virus.[23] In fact, studies reported that the Omicron variant containing R346K renders almost all current antibody therapy for COVID-19 ineffective.[27] Furthermore, these specific residues have also been observed in different Omicron sublineages, indicating a significant growth advantage.[31] Observing these trends, we selected 33 RBD mutations present in the spike of the XBB.1.5 subvariant for further structural analysis (Figure 5C). We compared the epitope mapping of mAbs 6D6 (Class 5), S2H97 (Class 5), and S309 (Class 3), based upon available information from complex structures[18] (Figure 5D). We identified only a single amino acid variation (N460→K) within the footprint of 6D6. Although 6D6 forms interactions with the main chain of N460 at the interface, the side chain alteration does not significantly affect the activity of 6D6 against XBB.1.5 (Figures 3A–3C, 5E, and 5F). Moreover, all 33 mutated amino acid sites are located outside the S2H97 epitope (Figure 5G). However, we discovered that three amino acid substitutions are present in the footprint of the S309 antibody (R339→D, R346→T, N440→K). These mutations may potentially impact the interaction of S309 with the Omicron
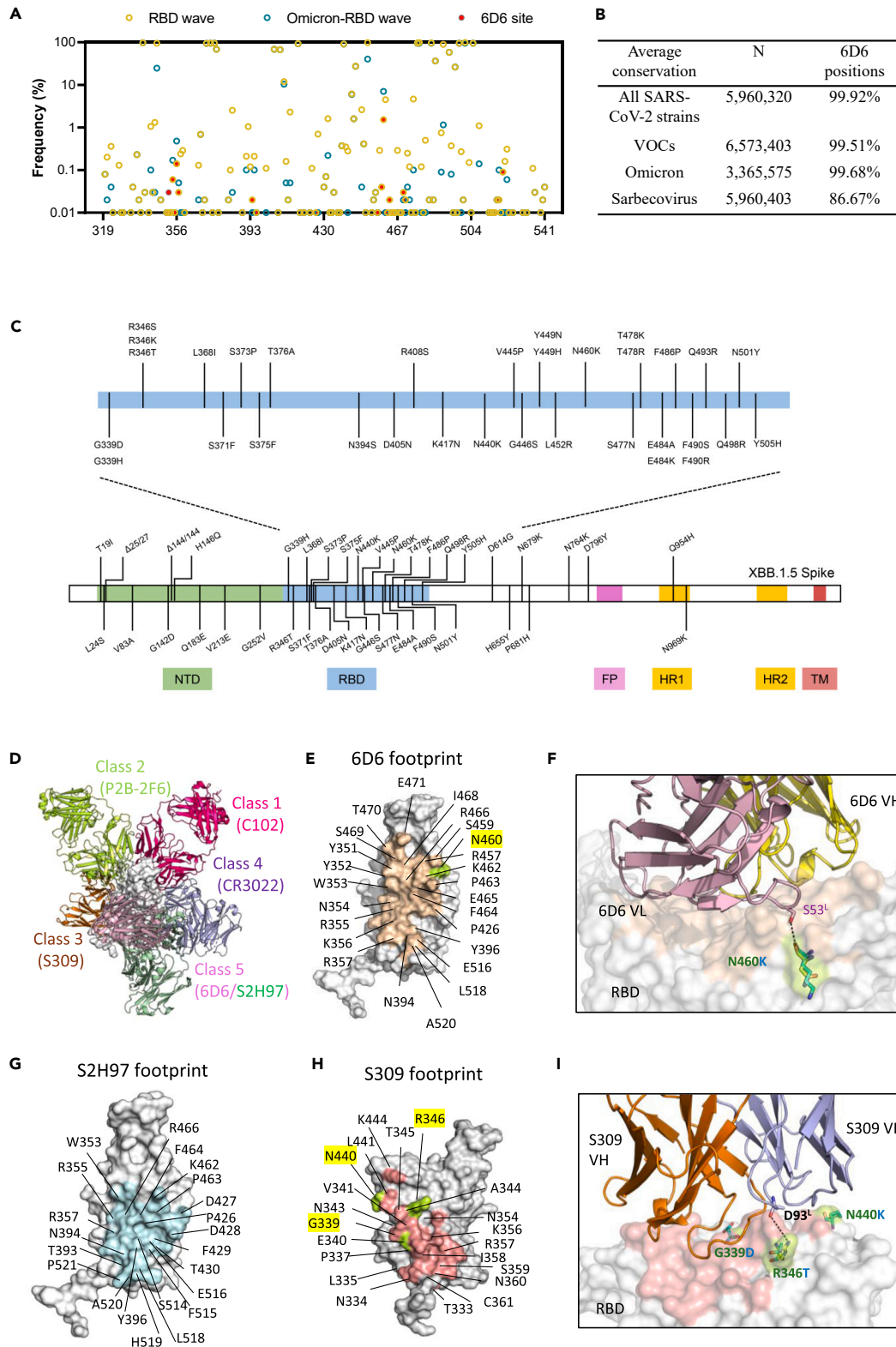
Figure 5. Structural illustration of 6D6 interaction with SARS-CoV-2 RBD

(A) Frequencies of amino acid substitutions observed at each codon of the SARS-CoV-2 RBD (aa 319–541) across various VOCs and Omicron pandemic waves. The amino acids of the 6D6 binding site are represented by red solid dots.

Figure 5. Continued

(B) The conservation of 6D6 epitopes in all SARS-CoV-2 strains (N = 5,960,320), SARS-CoV-2 VOCs including Alpha, Beta, Gamma, Delta, Lambda, Mu and Omicron (N = 6,573,403), Omicron(N = 3,365,575), *Sarbecovirus*(N = 5,960,403).

(C) Schematic representation of mutations presents in the spike protein of XBB.1.5 subvariant. A selected set of representative RBD mutations were chosen for functional assessment in this study.

(D) Overlay of RBD structures (gray) alongside Class 1–5 mAbs, C102 (PDB: 7K8M), P2B-2F6 (PDB: 7BWJ), S309 (PDB: 6WPS), CR3022 (PDB: 6YLA), 6D6 (PDB: 7EAN) and S2H97 (PDB: 7M7W), showcasing distinct binding orientations.

(E), (G) and (H) Residues on the RBD involved in interactions with 6D6, S2H97, and S309 are indicated. The mutated residue from (B) is highlighted in yellow.

(F) The interaction between 6D6 and two different RBD (WT RBD, PDB: 7EAN, XBB.1.5 RBD, PDB:8SPI) located at the interface.

(I) The interaction between S309 and two different RBD (WT RBD, PDB: 7EAN, XBB.1.5 RBD, PDB:8SPI) located at the interface.

lineage, further driving escape of XBB.1.5 from S309 (Figures 3A–3C, 5H, and 5I). Studies indicated that R346T and G339H mutations could cf. the strong neutralization resistance of these two subvariants to S309-like antibodies.[32] In summary, class 5 epitopes are highly conserved during viral evolution, and antibodies targeting class 5 epitope, represented by 6D6 and S2H97, are not affected by Omicron mutations. Combined with the neutralization analysis, 6D6 maintains its broad-spectrum neutralizing activity in the current wave of the Omicron variant, compared with another conserved epitope class 3, represented by S309. These findings present both a structural basis and experimental evidence for the broad-spectrum neutralizing epitope targeted by 6D6-like antibodies in the antigenicity evolution of SARS-CoV-2.

DISCUSSION

SARS-CoV-2 variants, particularly the Omicron variant, exhibit a high degree of adaptability, marked by an unprecedented number of mutations among VOCs. These mutations enhance transmissibility and immune evasion, significantly impacting the effectiveness of existing mAbs and vaccines. Consequently, Omicron represents a substantial public health challenge, complicating efforts to return to normalcy. In the face of continuously evolving SARS-CoV-2 variants, identifying conserved epitopes is crucial for developing universal vaccines and broadly neutralizing antibodies.

The 6D6 epitope is well conserved across divergent *Sarbecoviruses*. So far, few of the SARS-CoV-2 VOCs display mutations near the class 5 antigenic site, which suggests that the probability of viral mutation at the 6D6 epitope is quite low. We demonstrated broad recognition capability of 6D6, with high-affinity binding to S-6P from all tested variants. Notably, 6D6 effectively neutralized all known VOCs, including recent Omicron subvariants such as BA.1, BA.2, BA.4, BA.5, and XBB. Despite its moderate neutralizing activity, 6D6 showed stable IC_{50} values across variants, a rare attribute among current antibodies. The 6D6 caused dissociation of stabilized S-6P trimer, providing a strong, well-documented mechanism for the potent neutralizing activity. Additionally, *in vivo* studies in a hamster model infected with the Beta variant revealed efficacy of 6D6 in reducing viral load and mitigating lung pathology, resulting in 100% survival. Specifically, although S309 demonstrates relatively low affinity for BA.2 S-6P, it still provides superior neutralization against BA.2 when compared to 6D6. This discrepancy between affinity and neutralization outcomes suggests that the neutralization mechanism of 6D6, which involves the dissociation of the trimer, may be less effective than S309's mechanism by bivalent avidity effect despite not competing with receptor attachment like 6D6.[13] Nevertheless, the efficacy of 6D6 has conferred *in vivo* protection against beta SARS-CoV-2 in hamsters. The development of therapeutic antibodies could benefit from the cocktailing antibodies with diverse mechanism to maximize therapeutic efficacy. It is worth noting that this study did not evaluate the *in vivo* protective effect of 6D6 against the Omicron variant. However, considering the shared mutations between the beta and Omicron variants, as well as the lower pathogenicity of Omicron compared to beta, studying the efficacy of 6D6 against Omicron XBB in future would be valuable.[33–35]

To date, neutralizing antibodies have primarily targeted epitopes on the spike protein, predominantly on the RBD and, to a lesser extent, the NTD and S2 subunit. Previous structural and binding competition studies have shown that the most potently neutralizing anti-RBD antibodies target several distinct epitopes on the RBD.[24] Studies also highlight a trade-off between sarbecovirus breadth and potency against SARS-CoV-2.[18] Generally, mAbs targeting class 1–4 sites of the RBD, as well as those directed against the NTD, exhibit greater potency.[36] However, antibodies in these groups are highly susceptible to neutralization escape due to mutations and deletions found in emerging VOCs.[36] By contrast, mAbs targeting class 5 site exhibit broader activity and higher resistance to viral escape, yet they usually demonstrate lower potency.[18,36] The class 5 epitope remained conserved during the evolution of virus, which suggests that the probability of viral mutation at the class 5 epitope is quite low.[25] A few previously reported neutralizing antibodies, such as S2H97,[18] 553-49,[37] and XMA09,[17] targeting this site have shown remarkably broad neutralization. Mutation of the class 5 epitope by deep mutational scanning of the RBD showed that mutation of these residues predominantly resulted in decreased protein expression, ACE2 binding, and viral infectivity, denoting the functional and structural constraint of several class 5 epitope residues, particularly around E465.[38] Enhanced potency might be achieved through engineering mAbs that target the class 5 epitope as multivalent formats, making them key members of a variant-resistant cocktail. Notably, class 5 antibodies are less frequently reported than other classes. According to CoV-AbDab database, the heavy chain of representative class 5 human antibodies, S2H97 and WRAIR-2063, were encoded by the gene IGHV5-51 and IGH3-33, only 3.6% and 3.5% among the reported coronavirus antibodies using these genes, respectively, while 10% of heavy chain of class 1 antibodies were encoded by the IGHV3-53 gene.[25,39,40] These studies underscore the rarity and uniqueness of the VH genes usage by class 5 antibodies.

The epitopes targeted by neutralizing antibodies remain a pivotal focus in vaccine design and the development of therapeutic antibodies. We underscore the importance of targeting conserved viral epitopes to create antibody therapies with broad-spectrum

efficacy and to inform vaccine development. Glycan engineering is a strategy being tested to reduce the immunogenicity of regions outside the conserved epitopes. One potential approach is to introduce glycans into the spike or RBD of SARS-CoV-2, which can shield regions of low interest and enhance the exposure of desirable epitopes for broadly neutralizing antibodies.[41] Similarly, designing SARS-CoV-2 antigens to target the 6D6 epitope could stimulate the production of rare but broadly neutralizing antibodies. Additionally, cocktail treatments combining antibodies that target different epitope sites are expected to exhibit synergistic effects and reduce the chance of escape mutations. Indeed, combination of three noncompeting RBD-specific neutralizing antibodies (nAbs), such as REGN10933, REGN10987, and REGN10985, improved the efficiency of individual nAbs in neutralizing SARS-CoV-2 variants, preventing the development of escape mutants.[42] In addition, it had been reported that presence of some class 5 antibodies such as WRAIR-2063 can significantly enhance S protein binding to other mAbs with cryptic S protein epitopes.[25] The 6D6 exhibits considerable breadth, with a nearly invariant antigenic sites, and modest neutralization capacity. Thus, therapeutics incorporating it as one component of a cocktail may provide synergistic protection against SARS-CoV-2 variants and prevent viral escape, representing a more robust therapeutic option than what is presently available.

Given the likelihood of SARS-CoV-2 persisting in the human population, ongoing global genomic surveillance, enhanced vaccination campaigns, development of nAbs, and new drugs are crucial in the fight against COVID-19. The global effort has led to the development of broad vaccines, which continue to cf. immunity against currently circulating SARS-CoV-2 variants. By differentiating antibody epitopes with high resolution, as demonstrated in our study, we can inform the development of targeted antibodies and vaccines. The binding epitope of 6D6 within the sarbecovirus is a promising target for pan-sarbecovirus vaccine development. Furthermore, the *in vivo* protective efficacy data suggest that 6D6 could be a potential drug candidate for treating or preventing COVID-19 infection. Engineering 6D6 in a multivalent format may enhance its potency, making it a valuable addition to variant-resistant cocktail formulations in the future.

Limitations of the study

Due to the continuous evolution of SARS-CoV-2, the statistics on the conservation of the 6D6 epitope are limited to the documented SARS-CoV-2 isolates available at the time of writing. Consequently, continuous monitoring of the conservation of the 6D6 epitope is necessary.

STAR★METHODS

Detailed methods are provided in the online version of this paper and include the following:

- KEY RESOURCES TABLE
- RESOURCE AVAILABILITY
  - Lead contact
  - Materials availability
  - Data and code availability
- EXPERIMENTAL MODEL AND STUDY PARTICIPANT DETAILS
  - Cell cultures
- METHOD DETAILS
  - Expression and purification of mAbs
  - Expression and purification of S-6P proteins
  - SDS-PAGE
  - Enzyme-linked immunosorbent assay (ELISA)
  - Pseudotype LV-based neutralization assay
  - KD determination
  - Therapy against beta variants in hamsters
  - SARS-CoV-2 RNA quantification
- QUANTIFICATION AND STATISTICAL ANALYSIS

SUPPLEMENTAL INFORMATION

Supplemental information can be found online at https://doi.org/10.1016/j.isci.2024.110208.

![CellPress OPEN ACCESS logo]

AUTHOR CONTRIBUTIONS

DECLARATION OF INTERESTS

REFERENCES

1. Khan, M., Adil, S.F., Alkhathlan, H.Z., Tahir, M.N., Saif, S., Khan, M., and Khan, S.T. (2020). COVID-19: A Global Challenge with Old History, Epidemiology and Progress So Far. Molecules 26, 39. https://doi.org/10.3390/molecules26010039.

2. Giovanetti, M., Benedetti, F., Campisi, G., Ciccozzi, A., Fabris, S., Ceccarelli, G., Tambone, V., Caruso, A., Angeletti, S., Zella, D., and Ciccozzi, M. (2021). Evolution patterns of SARS-CoV-2: Snapshot on its genome variants. Biochem. Biophys. Res. Commun. 538, 88–91. https://doi.org/10.1016/j.bbrc.2020.10.102.

3. Muralidar, S., Ambi, S.V., Sekaran, S., and Krishnan, U.M. (2020). The emergence of COVID-19 as a global pandemic: Understanding the epidemiology, immune response and potential therapeutic targets of SARS-CoV-2. Biochimie 179, 85–100. https://doi.org/10.1016/j.biochi.2020.09.018.

4. Nimavat, N., Singh, S., Agrawal, A., Rafi, M.A., Bhatti, B., Parmar, G., and Shah, A. (2021). Mutations in SARS-CoV-2 genomes and future strategies. Clin. Epidemiol. Glob. Health 12, 100875. https://doi.org/10.1016/j.cegh.2021.100875.

5. Kumari, M., Lu, R.M., Li, M.C., Huang, J.L., Hsu, F.F., Ko, S.H., Ke, F.Y., Su, S.C., Liang, K.H., Yuan, J.P.Y., et al. (2022). A critical overview of current progress for COVID-19: development of vaccines, antiviral drugs, and therapeutic antibodies. J. Biomed. Sci. 29, 68. https://doi.org/10.1186/s12929-022-00852-9.

6. Chatterjee, B., and Thakur, S.S. (2022). Diverse vaccine platforms safeguarding against SARS-CoV-2 and its variants. Expert Rev. Vaccines 21, 47–67. https://doi.org/10.1080/14760584.2022.1997601.

7. Garcia-Beltran, W.F., St Denis, K.J., Hoelzemer, A., Lam, E.C., Nitido, A.D., Sheehan, M.L., Berrios, C., Ofoman, O., Chang, C.C., Hauser, B.M., et al. (2022). mRNA-based COVID-19 vaccine boosters induce neutralizing immunity against SARS-CoV-2 Omicron variant. Cell 185, 457–466.e4. https://doi.org/10.1016/j.cell.2021.12.033.

8. Wang, R., Huang, H., Yu, C., Sun, C., Ma, J., Kong, D., Lin, Y., Zhao, D., Zhou, S., Lu, J., et al. (2023). A spike-trimer protein-based tetravalent COVID-19 vaccine elicits enhanced breadth of neutralization against SARS-CoV-2 Omicron subvariants and other variants. Sci. China Life Sci. 66, 1818–1830. https://doi.org/10.1007/s11427-022-2207-7.

9. Wang, Q., Iketani, S., Li, Z., Liu, L., Guo, Y., Huang, Y., Bowen, A.D., Liu, M., Wang, M., Yu, J., et al. (2023). Alarming antibody evasion properties of rising SARS-CoV-2 BQ and XBB subvariants. Cell 186, 279–286.e8. https://doi.org/10.1016/j.cell.2022.12.018.

10. Levin, M.J., Ustianowski, A., De Wit, S., Launay, O., Avila, M., Seegobin, S., Templeton, A., Yuan, Y., Ambery, P., Arends, R.H., et al. (2021). LB5. PROVENT: Phase 3 Study of Efficacy and Safety of AZD7442 (Tixagevimab/Cilgavimab) for Pre-exposure Prophylaxis of COVID-19 in Adults. Open Forum Infect. Dis. 8, S810. https://doi.org/10.1093/fofid/fofab466.1646.

11. VanBlargan, L.A., Errico, J.M., Halfmann, P.J., Zost, S.J., Crowe, J.E., Jr., Purcell, L.A., Kawaoka, Y., Corti, D., Fremont, D.H., and Diamond, M.S. (2022). An infectious SARS-CoV-2 B.1.1.529 Omicron virus escapes neutralization by therapeutic monoclonal antibodies. Nat. Med. 28, 490–495. https://doi.org/10.1038/s41591-021-01678-y.

12. Hansen, J., Baum, A., Pascal, K.E., Russo, V., Giordano, S., Wloga, E., Fulton, B.O., Yan, Y., Koon, K., Patel, K., et al. (2020). Studies in humanized mice and convalescent humans yield a SARS-CoV-2 antibody cocktail. Science 369, 1010–1014. https://doi.org/10.1126/science.abd0827.

13. Pinto, D., Park, Y.J., Beltramello, M., Walls, A.C., Tortorici, M.A., Bianchi, S., Jaconi, S., Culap, K., Zatta, F., De Marco, A., et al. (2020). Cross-neutralization of SARS-CoV-2 by a human monoclonal SARS-CoV antibody. Nature 583, 290–295. https://doi.org/10.1038/s41586-020-2349-y.

14. Mistry, P., Barmania, F., Mellet, J., Peta, K., Strydom, A., Viljoen, I.M., James, W., Gordon, S., and Pepper, M.S. (2021). SARS-CoV-2 Variants, Vaccines, and Host Immunity. Front. Immunol. 12, 809244. https://doi.org/10.3389/fimmu.2021.809244.

15. Jackson, C.B., Farzan, M., Chen, B., and Choe, H. (2022). Mechanisms of SARS-CoV-2 entry into cells. Nat. Rev. Mol. Cell Biol. 23, 3–20. https://doi.org/10.1038/s41580-021-00418-x.

16. Barnes, C.O., Jette, C.A., Abernathy, M.E., Dam, K.-M.A., Esswein, S.R., Gristick, H.B., Malyutin, A.G., Sharaf, N.G., Huey-Tubman, K.E., Lee, Y.E., et al. (2020). SARS-CoV-2 neutralizing antibody structures inform therapeutic strategies. Nature 588, 682–687. https://doi.org/10.1038/s41586-020-2852-1.

17. Wang, S., Sun, H., Zhang, Y., Yuan, L., Wang, Y., Zhang, T., Wang, S., Zhang, J., Yu, H., Xiong, H., et al. (2022). Three SARS-CoV-2 antibodies provide broad and synergistic neutralization against variants of concern, including Omicron. Cell Rep. 39, 110862. https://doi.org/10.1016/j.celrep.2022.110862.

18. Starr, T.N., Czudnochowski, N., Liu, Z., Zatta, F., Park, Y.-J., Addetia, A., Pinto, D., Beltramello, M., Hernandez, P., Greaney, A.J., et al. (2021). SARS-CoV-2 RBD antibodies that maximize breadth and resistance to escape. Nature 597, 97–102. https://doi.org/10.1038/s41586-021-03807-6.

19. Ai, J., Wang, X., He, X., Zhao, X., Zhang, Y., Jiang, Y., Li, M., Cui, Y., Chen, Y., Qiao, R., et al. (2022). Antibody evasion of SARS-CoV-2 Omicron BA.1, BA.1.1, BA.2, and BA.3 sub-lineages. Cell Host Microbe 30, 1077–1083.e4. https://doi.org/10.1016/j.chom.2022.05.001.

20. Chen, Y., Zhao, X., Zhou, H., Zhu, H., Jiang, S., and Wang, P. (2023). Broadly neutralizing antibodies to SARS-CoV-2 and other human coronaviruses. Nat. Rev. Immunol. 23, 189–199. https://doi.org/10.1038/s41577-022-00784-3.

21. Planas, D., Saunders, N., Maes, P., Guivel-Benhassine, F., Planchais, C., Buchrieser, J., Bolland, W.-H., Porrot, F., Staropoli, I., Lemoine, F., et al. (2022). Considerable escape of SARS-CoV-2 Omicron to antibody neutralization. Nature 602, 671–675. https://doi.org/10.1038/s41586-021-04389-z.

22. Ao, D., He, X., Hong, W., and Wei, X. (2023). The rapid rise of SARS-CoV-2 Omicron subvariants with immune evasion properties: XBB.1.5 and BQ.1.1 subvariants. MedComm (2020) 4, e239. https://doi.org/10.1002/mco2.239.

23. Li, T., Xue, W., Zheng, Q., Song, S., Yang, C., Xiong, H., Zhang, S., Hong, M., Zhang, Y., Yu, H., et al. (2021). Cross-neutralizing antibodies bind a SARS-CoV-2 cryptic site and resist circulating variants. Nat. Commun. 12, 5652. https://doi.org/10.1038/s41467-021-25997-3.

24. Dejnirattisai, W., Zhou, D., Ginn, H.M., Duyvesteyn, H.M.E., Supasa, P., Case, J.B., Zhao, Y., Walter, T.S., Mentzer, A.J., Liu, C., et al. (2021). The antigenic anatomy of SARS-CoV-2 receptor binding domain. Cell 184, 2183–2200.e22. https://doi.org/10.1016/j.cell.2021.02.032.

25. Jensen, J.L., Sankhala, R.S., Dussupt, V., Bai, H., Hajduczki, A., Lal, K.G., Chang, W.C., Martinez, E.J., Peterson, C.E., Golub, E.S., et al. (2023). Targeting the Spike Receptor Binding Domain Class V Cryptic Epitope by an Antibody with Pan-Sarbecovirus Activity.

J. Virol. *97*, e0159622. https://doi.org/10.1128/jvi.01596-22.

26. Liu, L., Iketani, S., Guo, Y., Reddem, E.R., Casner, R.G., Nair, M.S., Yu, J., Chan, J.F.W., Wang, M., Cerutti, G., et al. (2022). An antibody class with a common CDRH3 motif broadly neutralizes sarbecoviruses. Sci. Transl. Med. *14*, eabn6859. https://doi.org/10.1126/scitranslmed.abn6859.

27. Liu, L., Iketani, S., Guo, Y., Chan, J.F.W., Wang, M., Liu, L., Luo, Y., Chu, H., Huang, Y., Nair, M.S., et al. (2022). Striking antibody evasion manifested by the Omicron variant of SARS-CoV-2. Nature *602*, 676–681. https://doi.org/10.1038/s41586-021-04388-0.

28. Lempp, F.A., Soriaga, L.B., Montiel-Ruiz, M., Benigni, F., Noack, J., Park, Y.J., Bianchi, S., Walls, A.C., Bowen, J.E., Zhou, J., et al. (2021). Lectins enhance SARS-CoV-2 infection and influence neutralizing antibodies. Nature *598*, 342–347. https://doi.org/10.1038/s41586-021-03925-1.

29. Tao, K., Tzou, P.L., Nouhin, J., Gupta, R.K., de Oliveira, T., Kosakovsky Pond, S.L., Fera, D., and Shafer, R.W. (2021). The biological and clinical significance of emerging SARS-CoV-2 variants. Nat. Rev. Genet. *22*, 757–773. https://doi.org/10.1038/s41576-021-00408-x.

30. Abu-Raddad, L.J., Chemaitelly, H., Ayoub, H.H., Yassine, H.M., Benslimane, F.M., Al Khatib, H.A., Tang, P., Hasan, M.R., Coyle, P., AlMukdad, S., et al. (2022). Severity, Criticality, and Fatality of the Severe Acute Respiratory Syndrome Coronavirus 2 (SARS-CoV-2) Beta Variant. Clin. Infect. Dis. *75*, e1188–e1191. https://doi.org/10.1093/cid/ciab909.

31. Cao, Y., Jian, F., Wang, J., Yu, Y., Song, W., Yisimayi, A., Wang, J., An, R., Chen, X., Zhang, N., et al. (2023). Imprinted SARS-CoV-2 humoral immunity induces convergent Omicron RBD evolution. Nature *614*, 521–529. https://doi.org/10.1038/s41586-022-05644-7.

32. Qu, P., Faraone, J.N., Evans, J.P., Zheng, Y.M., Carlin, C., Anghelina, M., Stevens, P., Fernandez, S., Jones, D., Panchal, A.R., et al. (2023). Enhanced evasion of neutralizing antibody response by Omicron XBB.1.5, CH.1.1, and CA.3.1 variants. Cell Rep. *42*, 112443. https://doi.org/10.1016/j.celrep.2023.112443.

33. Weng, S., Shang, J., Cheng, Y., Zhou, H., Ji, C., Yang, R., and Wu, A. (2022). Genetic differentiation and diversity of SARS-CoV-2 Omicron variant in its early outbreak. Biosaf. Health *4*, 171–178. https://doi.org/10.1016/j.bsheal.2022.04.004.

34. McMahan, K., Giffin, V., Tostanoski, L.H., Chung, B., Siamatu, M., Suthar, M.S., Halfmann, P., Kawaoka, Y., Piedra-Mora, C., Jain, N., et al. (2022). Reduced pathogenicity of the SARS-CoV-2 omicron variant in hamsters. Med *3*, 262–268.e4. https://doi.org/10.1016/j.medj.2022.03.004.

35. Shuai, H., Chan, J.F.W., Hu, B., Chai, Y., Yuen, T.T.T., Yin, F., Huang, X., Yoon, C., Hu, J.C., Liu, H., et al. (2022). Attenuated replication and pathogenicity of SARS-CoV-2 B.1.1.529 Omicron. Nature *603*, 693–699. https://doi.org/10.1038/s41586-022-04442-5.

36. Hastie, K.M., Li, H., Bedinger, D., Schendel, S.L., Dennison, S.M., Li, K., Rayaprolu, V., Yu, X., Mann, C., Zandonatti, M., et al. (2021). Defining variant-resistant epitopes targeted by SARS-CoV-2 antibodies: A global consortium study. Science *374*, 472–478. https://doi.org/10.1126/science.abh2315.

37. Zhan, W., Tian, X., Zhang, X., Xing, S., Song, W., Liu, Q., Hao, A., Hu, Y., Zhang, M., Ying, T., et al. (2022). Structural Study of SARS-CoV-2 Antibodies Identifies a Broad-Spectrum Antibody That Neutralizes the Omicron Variant by Disassembling the Spike Trimer. J. Virol. *96*, e0048022. https://doi.org/10.1128/jvi.00480-22.

38. Starr, T.N., Greaney, A.J., Hilton, S.K., Ellis, D., Crawford, K.H.D., Dingens, A.S., Navarro, M.J., Bowen, J.E., Tortorici, M.A., Walls, A.C., et al. (2020). Deep Mutational Scanning of SARS-CoV-2 Receptor Binding Domain Reveals Constraints on Folding and ACE2 Binding. Cell *182*, 1295–1310.e20. https://doi.org/10.1016/j.cell.2020.08.012.

39. Raybould, M.I.J., Kovaltsuk, A., Marks, C., and Deane, C.M. (2021). CoV-AbDab: the coronavirus antibody database. Bioinformatics *37*, 734–735. https://doi.org/10.1093/bioinformatics/btaa739.

40. Yuan, M., Liu, H., Wu, N.C., Lee, C.C.D., Zhu, X., Zhao, F., Huang, D., Yu, W., Hua, Y., Tien, H., et al. (2020). Structural basis of a shared antibody response to SARS-CoV-2. Science *369*, 1119–1123. https://doi.org/10.1126/science.abd2321.

41. Martina, C.E., Crowe, J.E., Jr., and Meiler, J. (2023). Glycan masking in vaccine design: Targets, immunogens and applications. Front. Immunol. *14*, 1126034. https://doi.org/10.3389/fimmu.2023.1126034.

42. Copin, R., Baum, A., Wloga, E., Pascal, K.E., Giordano, S., Fulton, B.O., Zhou, A., Negron, N., Lanza, K., Chan, N., et al. (2021). The monoclonal antibody combination REGEN-COV protects against SARS-CoV-2 mutational escape in preclinical and human studies. Cell *184*, 3949–3961.e11. https://doi.org/10.1016/j.cell.2021.06.002.

43. Shi, R., Shan, C., Duan, X., Chen, Z., Liu, P., Song, J., Song, T., Bi, X., Han, C., Wu, L., et al. (2020). A human neutralizing antibody targets the receptor-binding site of SARS-CoV-2. Nature *584*, 120–124. https://doi.org/10.1038/s41586-020-2381-y.

44. Zhang, Y., Wei, M., Wu, Y., Wang, J., Hong, Y., Huang, Y., Yuan, L., Ma, J., Wang, K., Wang, S., et al. (2022). Cross-species tropism and antigenic landscapes of circulating SARS-CoV-2 variants. Cell Rep. *38*, 110558. https://doi.org/10.1016/j.celrep.2022.110558.

45. Chang, L., Hou, W., Zhao, L., Zhang, Y., Wang, Y., Wu, L., Xu, T., Wang, L., Wang, J., Ma, J., et al. (2021). The prevalence of antibodies to SARS-CoV-2 among blood donors in China. Nat. Commun. *12*, 1383. https://doi.org/10.1038/s41467-021-21503-x.

46. Wu, Y., Huang, X., Yuan, L., Wang, S., Zhang, Y., Xiong, H., Chen, R., Ma, J., Qi, R., Nie, M., et al. (2021). A recombinant spike protein subunit vaccine confers protective immunity against SARS-CoV-2 infection and transmission in hamsters. Sci. Transl. Med. *13*, eabg1143. https://doi.org/10.1126/scitranslmed.abg1143.

STAR★METHODS

KEY RESOURCES TABLE

REAGENT or RESOURCE	SOURCE	IDENTIFIER
Antibodies		
6D6	Li et al.[23]	N/A
S309	Pinto et al.[13]	RRID: AB_2941328
CB6	Shi et al.[43]	N/A
RENG10933	Hansen et al.[12]	N/A
Bacterial and virus strains		
SARS-CoV-2 D614G pseudovirus (LV)	Zhang et al.[44]	N/A
SARS-CoV-2 B.1.617.1 pseudovirus (LV)	Zhang et al.[44]	N/A
SARS-CoV-2 B.1.617.2 pseudovirus (LV)	Zhang et al.[44]	N/A
SARS-CoV-2 BA.1 pseudovirus (LV)	Zhang et al.[44]	N/A
SARS-CoV-2 BA.1.1 pseudovirus (LV)	Zhang et al.[44]	N/A
SARS-CoV-2 BA.2 pseudovirus (LV)	Zhang et al.[44]	N/A
SARS-CoV-2 BA.2.12.1 pseudovirus (LV)	Zhang et al.[44]	N/A
SARS-CoV-2 BA.2.75 pseudovirus (LV)	Zhang et al.[44]	N/A
SARS-CoV-2 BA.4 pseudovirus (LV)	Zhang et al.[44]	N/A
SARS-CoV-2 BA.5 pseudovirus (LV)	Zhang et al.[44]	N/A
SARS-CoV-2 BF.7 pseudovirus (LV)	Zhang et al.[44]	N/A
SARS-CoV-2 BQ.1.1 pseudovirus (LV)	Zhang et al.[44]	N/A
SARS-CoV-2 XBB.1 pseudovirus (LV)	Zhang et al.[44]	N/A
SARS-CoV-2 XBB.1.5 pseudovirus (LV)	Zhang et al.[44]	N/A
Chemicals, peptides, and recombinant proteins		
SARS-CoV-2 D614G S-6P	This manuscript	N/A
SARS-CoV-2 B.1.621 S-6P	This manuscript	N/A
SARS-CoV-2 C.1.2 S-6P	This manuscript	N/A
SARS-CoV-2 B.1.617.2 S-6P	This manuscript	N/A
SARS-CoV-2 B.1.529 S-6P	This manuscript	N/A
SARS-CoV-2 BA.2 S-6P	This manuscript	N/A
SARS-CoV-2 B.1.640.1 S-6P	This manuscript	N/A
SARS-CoV-2 XBB.1.5 S-6P	This manuscript	N/A
SARS-CoV S-6P	This manuscript	N/A
Critical commercial assays		
Ni Sepharose 6 Fast Flow	Cytiva	Cat#17-5318-03
MabSelect SuRe	Cytiva	Cat#17-5438-02
SARS-CoV-2 RT-PCR Kit	Wantai	Cat#WS-1248
QIAamp Viral RNA Mini Kit	Qiagen	Cat#52906
ExpiCHO Expression Medium	Thermo Fisher Scientific	Cat#A2910002
ExpiFectamine CHO Transfection Kit	Thermo Fisher Scientific	Cat#A29129
OPM-293 CD05 Medium	OPM	Cat#81075-001
PEI MW40000 transfection reagent	YEASEN	Cat# 40816ES03

(Continued on next page)

Continued

REAGENT or RESOURCE	SOURCE	IDENTIFIER
Experimental models: Cell lines		
Expi293F cells	Thermo Fisher Scientific	Cat#A14528
ExpiCHO cells	Thermo Fisher Scientific	Cat#A29127
H1299-ACE2hR	Zhang et al.[44]	N/A
293T	Zhang et al.[44]	N/A
Vero cells	ATCC	Cat#CCL-81
Experimental models: Organisms/strains		
LVG Syrian hamsters	Charles River	Cat#501
Software and algorithms		
GraphPad Prism (version 8.0.1)	Graphpad	https://www.graphpad.com/
PyMOL	PyMOL	https://pymol.org/

RESOURCE AVAILABILITY

Lead contact

Information and requests for resources should be directed to and will be fulfilled by the lead contact, Shaowei Li (shaowei@xmu.edu.cn).

Materials availability

All plasmids generated in this study are available from the lead contact without restriction.

Data and code availability

- All data reported in this paper will be shared by the lead contact upon request.
- This paper does not report original code.
- Any additional information required to reanalyze the data reported in this paper is available from the lead contact upon request.

EXPERIMENTAL MODEL AND STUDY PARTICIPANT DETAILS

Cell cultures

Cell lines used in this study were sourced from Thermo Fisher Scientific Inc. Chinese Hamster Ovary, CHO, were cultured in ExpiCHO™ Expression Medium. Human embryonic kidney cells, HEK293F, were maintained in OPM-293 CD05 Medium. Cells were cultured at 37°C, 5% CO2 at 95% air atmosphere. All cell lines used in this study were routinely tested for mycoplasma and found to be mycoplasma-free.

METHOD DETAILS

Expression and purification of mAbs

The isolation and purification of 6D6 were described by us elsewhere.[23] The variable domain genes of S309,[13] CB6[43] and REGN10933[12] heavy and light chains were cloned into a pTT5 (Thermo Fisher Scientific) vector containing the constant region of the human IgG. The recombinant antibodies were expressed in Chinese hamster ovary (CHO) cells through transient transfection with equal amounts of paired heavy and light chain plasmids. Antibodies in the culture supernatant were purified by affinity chromatography using protein A agarose columns (Cytiva).

Expression and purification of S-6P proteins

The SARS-CoV-2 D614G S-6P proteins carrying six stabilizing Pro substitutions (817, 892, 899, 942, 986, and 987) and ''GSAS'' substitutions at the furin cleavage site (682–685). The coding genes of spike ectodomain followed by a foldon trimerization motif, a His tag, and a flag tag at the C-terminus were synthesized and cloned into the pcDNA3.4 vector by GenScript. All S-6P plasmids, containing D614G, B.1.621 (Mu), C.1.2, B.1.617.2 (Delta), B.1.1.529 (Omicron), BA.2, B.1.640.1, XBB.1.5, SARS-CoV, were transiently transfected into 293 F cells, respectively. After 6 days, the secreted S-6P proteins were purified from the supernatant using Ni-sepharose fast-flow 6 resin (Cytiva) and eluted with 250 mM imidazole.

SDS-PAGE

Protein samples were prepared with loading buffer, boiled for 10 min, and subjected to sodium dodecyl sulfate-polyacrylamide gel electrophoresis (SDS-PAGE). Equal amounts of protein for each sample were loaded onto SDS-PAGE gels and electrophoresed at 160 V for

45 minutes using a BioRad MINI-PROTEAN Tetra system (BioRad Laboratories, CA, USA). The gels were stained with Coomassie Brilliant Blue R-250 (Bio-Rad) for 20 min at room temperature.

Enzyme-linked immunosorbent assay (ELISA)

Purified proteins (200 ng/well) were coated onto 96-well microtitre plates and incubated at 37°C for 2 hours. Plates were blocked with 1 × enzyme dilution buffer (PBS + 0.25% casein + 1% gelatin + 0.05% proclin-300) at 37°C for 2 hours. Antibodies (2 μg/mL) were serially diluted, added to the wells (100 μL), and incubated at 37°C for 30 minutes. A horseradish peroxidase (HRP)-labeled goat anti-mouse or mouse anti-human antibody (Abcam) was used as the secondary antibody at 1:5000 dilution. After washing, the reaction was developed using o-phenylenediamine substrate at 37°C for 10 min. The OD_{450nm} (reference OD_{620nm}) was measured on a microplate reader (TECAN, Männedorf, Switzerland). The half-effective concentration (EC_{50}) values were calculated via sigmoid trend fitting with GraphPad Prism software (GraphPad Software, CA, USG).

Pseudotype LV-based neutralization assay

Antibodies were tested against lenti-viral pseudotyping particles (LVpp) bearing the SARS-CoV-2 spike antigen based on H1299-ACE2hR cells, as described previously.[45] In brief, SARS-CoV-2 LVpp were generated by co-transfection of a lentiviral packaging plasmid (psPAX2, Addgene), a SARS-CoV-2 spike expression plasmid (containing codon-optimized spike gene derived from the strain of D614G or B.1.617.1, B.1.617.2, BA.1, BA.1.1, BA.2, BA.2.12.1, BA.2.75, BA.4, BA.5, BF.7, BQ.1.1, XBB.1, XBB.1.5 and a green fluorescent protein (mNeon-Green) reporter vector (pLvEF1α-mNG, carrying EF1α promoter-driven mNeonGreen expressing cassette) in HEK293T cells. Infection and neutralization assays were performed on H1299-ACE2hR cells, which stably over-expressed human ACE2 (enabling it to be highly susceptible to SARS-CoV-2 virus) and nuclear-localized RFP (H2B-mRuby3, allowing accurate cell counting) based on H1299 cells. For ppNAT tests, serially diluted antibodies were incubated with LVpp inoculum (0.5 TU/cell) for 1 h. Subsequently, the mixtures were incubated with the cells, which had been pre-seeded in 96-well cell culture plates with an optically clear bottom. After 36 hours incubation, the plates were imaged by using Opera Phenix or Operetta CLS high-content equipment (PerkinElmer). For quantitative determination, fluorescence images were analyzed by Columbus Software 2.5.0 (Perki-nElmer), the numbers of mNeonGreen (+) cells per well were calculated to indicate the infection performance, and the total cell numbers per well were also counted to normalize the readouts. The reduction (%) on mNeonGreen (+) cells of the plasma-treated well in comparison with control-well was calculated to show the neutralization activity. The ppNAT titer of each sample was expressed as the maximum dilution concentration required to achieve infection inhibition by 50% (IC_{50}). The IC_{50} value was determined by the 4-parameter logistic (4PL) regression using GraphPad Prism software (GraphPad Software, CA, USG).

KD determination

KD values were determined by SPR technology using a Biacore 8K instrument (Cytiva). The S-6P was amine-coupled to a CM-5 sensor chip. Antibodies were then captured on the sensor surface at a flow rate of 30μl/min in PBS-P + buffer (0.2 M phosphate buffer with 27 mM KCl, 1.37 M NaCl, and 0.5% Surfactant P20 (Tween 20)). The antibodies were tested using serially diluted concentrations (200, 100, 50, 25, 12.5, 6.25, 0 nM). The flow durations were 200 s for the association stage and 10 min for dissociation. Association rates (ka), dissociation rates (kd), and affinity constants (KD) were calculated using BIAcore evaluation software.

Therapy against beta variants in hamsters

The therapeutic activity of antibodies against SARS-CoV-2 Beta variant strain (GISAID: EPI_ISL_2,779,639) that was passaged on Vero cells (#CCL-81, ATCC) in vivo were performed in a Syrian hamster model.[46] Groups of 8-week-old male hamsters were intranasally challenged with 1x10^4 PFU of SARS-CoV-2 Beta variant. After 24 h, the infected hamsters were treated intraperitoneally with 6D6 at 20 mg/kg dose or PBS. The health status and body weight changes were monitored daily. The lung tissues of hamsters were collected at 5 days post-infection (dpi). The therapeutic efficacy of 6D6 was determined depending on the indicators including body weight, tissue viral RNA load, and lung pathological examination in gross.

SARS-CoV-2 RNA quantification

The tissue samples including lung, trachea and nasal turbinate were separated from infected hamsters and homogenized with TissueLyser II (Qiagen), and SARS-CoV-2 RNA was extracted using the QIAamp Viral RNA Mini Kit (Qiagen). Then, the viral RNA concentration was quantified using a SARS-CoV-2 RT-PCR Kit (WS-1248, Wantai BioPharm) according to the manufacturer's instruction.

QUANTIFICATION AND STATISTICAL ANALYSIS

GraphPad Prism was used for all statistical calculations. EC_{50} and IC_{50} values were calculated by non-linear regression analysis [log(agonist) vs. response— variable slope (four parameters)]. Data are expressed as means ± SEM. Significant differences between groups were analysed by two-way ANOVA with Bonferroni's multiple comparisons test. *: $p < 0.05$; **: $p < 0.01$; ***: $p < 0.001$; ****: $p < 0.0001$.